Evaluation of dapsone and its synthetic derivative DDS-13 in cancer *in vitro*

GRISELDA A. CABRAL-PACHECO[1], VIRGINIA FLORES-MORALES[2], IDALIA GARZA-VELOZ[1], MIRIAM DAMIÁN-SANDOVAL[1], ROSA B. MARTÍNEZ-FLORES[1], MARÍA C. MARTÍNEZ-VÁZQUEZ[1], IVÁN DELGADO-ENCISO[3,4], IRAM P. RODRIGUEZ-SANCHEZ[5] and MARGARITA L. MARTINEZ-FIERRO[1]

[1]Molecular Medicine Laboratory, Academic Unit of Human Medicine and Health Sciences; [2]Laboratory of Asymmetric Synthesis and Bio-Chemoinformatics, Chemical Engineering, Autonomous University of Zacatecas, Zacatecas 98160; [3]School of Medicine, University of Colima, Colima 28040; [4]Cancerology State Institute, Colima State Health Services, Colima 28085; [5]Molecular and Structural Physiology Laboratory, School of Biological Sciences, Autonomous University of Nuevo Leon, Nuevo León 66455, Mexico

Received July 4, 2023; Accepted November 2, 2023

DOI: 10.3892/etm.2023.12335

Abstract. The present study highlighted the repositioning of the drug dapsone (DDS) for cancer therapy. Due to its mechanism of action, DDS has a dual effect as an antibiotic and as an anti-inflammatory/immunomodulator; however, at high doses, it has important adverse effects. The derivative DDS-13 [N,N'-(sulfonyl bis (4,1-phenylene)) dioctanamide] was synthesized through an N-acylation reaction to compare it with DDS. Its cytotoxic effects in cancer cells (DU145 and HeLa) and non-cancer cells (HDFa) were observed at concentrations ranging 0.01-100 μM and its physicochemical/pharmacokinetic properties were analyzed using the SwissADME tool. The objectives of the present study were to evaluate the anticancer activity of both DDS and DDS-13 and to identify the physicochemical and pharmacokinetic properties of DDS-13. The results showed that DDS-13 presented a cytotoxic effect in the DU145 cell line (IC_{50}=19.06 μM), while DDS showed a cytotoxic effect on both the DU145 (IC_{50}=11.11 μM) and HeLa (IC_{50}=13.07 μM) cell lines. DDS-13 appears to be a good cytotoxic candidate for the treatment of prostate cancer, while DDS appears to be a good candidate for both cervical and prostate cancer. Neither candidate showed a cytotoxic effect in non-cancerous cells. The different pharmacokinetic properties of DDS-13 make it a new candidate for evaluation in preclinical models for the treatment of cancer.

Correspondence to: Dr Virginia Flores-Morales, Laboratory of Asymmetric Synthesis and Bio-Chemoinformatics, Chemical Engineering, Autonomous University of Zacatecas, Campus XXI Km 6, Zacatecas-Guadalajara Highway, Zacatecas 98160, Mexico
E-mail: virginia.flores@uaz.edu.mx

Dr Margarita L. Martinez-Fierro, Molecular Medicine Laboratory, Academic Unit of Human Medicine and Health Sciences. Autonomous University of Zacatecas, Campus XXI Km 6, Zacatecas-Guadalajara Highway, Zacatecas 98160, Mexico
E-mail: margaritamf@uaz.edu.mx

Key words: dapsone, cancer, synthetic derivative, cytotoxicity, *in vitro* model

Introduction

Cancer is one of the greatest challenges to public health, as it has been the leading cause of mortality for several decades (1). Worldwide, cervical and prostate cancers represent two cancers with high incidence in women and men, respectively (2). The introduction of early detection strategies and improvements in cancer therapy have made it possible, in developed countries, to reduce the incidence of cancer and improve patient survival (1); however, current treatments are expensive and have serious adverse effects (3). Due to the aforementioned, the search for new treatments has increased considerably and new proposals have focused on developing more effective treatments with fewer adverse effects and with greater accessibility for the population. Drug repositioning is important for optimizing the preclinical process of new drug development, as it saves time and costs compared with traditional processes for *de novo* drug discovery (4). The purpose of synthesizing new compounds from existing drugs, such as dapsone (DDS), is to improve their activity and reduce their adverse effects. In 1961, Ross (5) first suggested the use of DDS as a safer and cheaper option compared with other systemic antibiotics for the treatment of acne vulgaris and recommended an oral dose of 50-150 mg of DDS per day, which showed no side effects after seven days (5). DDS is also recognized for treating leprosy and is used for a variety of other dermatological conditions, including dermatitis herpetiformis (6). As an antibacterial drug, DDS inhibits the synthesis of dihydrofolic acid through the inhibition of *para*-aminobenzoic acid at the dihydropteroate synthetase active site (7). In acne vulgaris, in addition to its antimicrobial effect, DDS has an anti-inflammatory effect (8) and has been found to inhibit chemoattractant signaling (9-11). Some evidence also suggests that DDS might have inhibitory

effects on myeloperoxidase in neutrophils, causing inflammation and tissue damage (7). According to the Biopharmaceutics Classification System (BCS), DDS is classified as a class II lipophilic drug with low solubility and high permeability (12) and, at high doses, it has significant adverse effects, such as hemolysis and methemoglobinemia (13). To date, there have been few studies evaluating the effects of DDS on types of cancer. An *in vitro* study highlighted DDS as an adjunct in the treatment of glioblastoma, possibly by blocking neutrophil migration to the tumor directed by low IL-8 and VEGF expressions, as well as low leukotriene synthesis (11). In the present study, the synthetic derivative of DDS (DDS-13) was selected because it has not been tested biologically or functionally to evaluate its pharmacological properties against other types of cancer. Therefore, the present study focused on evaluating the anticancer effects of DDS and its synthetic derivative DDS-13 in an *in vitro* study. The chemical structures of the compounds are shown in the results section (Fig. 1).

Materials and methods

Chemistry

Reagents. DDS (CAS 80-08-0), methyl caprylate (CAS 111-11-5) and triethylamine (CAS 121-44-8) were purchased from MilliporeSigma and used without prior purification. All of the solvents which were used were ACS-grade and purchased from J.T. Baker, Inc. The solvents were dried and purified in accordance with standard procedures (14). The microwave-assisted synthesis was performed using a CEM Discovery BenchMate apparatus (CEM Corporation). Iodine vapor was used as a detecting agent. The melting points were measured by means of Dynalon Afon DMP100 apparatus (Dynalab Corp.) and reported without correction. ^{1}H and ^{13}C nuclear magnetic resonance (NMR) experiments were recorded (dissolving the sample in 0.5 ml od acetone-d_6) on a 500 MHz Bruker Advance III (Bruker Corporation) with a pulse field gradient at 500 MHz for ^{1}H and 125 MHz for ^{13}C. Chemical shifts are given in values of ppm, referenced to tetramethylsilane as an internal standard. The coupling patterns are expressed as singulete (*s*), doublet (*d*), or a combination of the two. Fourier-transform infrared spectroscopy (FT-IR) was performed using a PerkinElmer 1320 (PerkinElmer, Inc.) with a sodium chloride cell.

Synthesis of the DDS-derived compound. The derivative DDS-13 was selected as a potential candidate from a group of dapsone-derived compounds with different characteristics and chemical properties (data not shown), which was synthesized by our research group. To obtain DDS-13, an *N*-acylation reaction was carried out using a procedure reported by Lidstrom *et al* (3rd edition) (15). In a 25 ml round flask containing a magnetic stir bar, DDS (1.2 mmol) was dissolved in 3 ml of acetone and Et_3N (2.0 mmol) was added dropwise while stirring for 30 min at room temperature. Then, methyl caprylate (0.08 mmol) was added. The mixture was heated to 70˚C using 100 W of power for 5 h. The solvent was removed using a rotary evaporator and the solid was crystallized using a hexane:acetone (8:2) system. The reaction was monitored using thin-layer chromatography on Merck silica gel 60 F_{254} plates (MilliporeSigma).

N,N'-(sulfonylbis(4,1-phenylene))dioctanamide (DDS-13) resulted in an amorphous white solid with a 75% yield; m.p. 158-160˚C. IR (υ, cm^{-1}): 3233, 3060, 1912, 1626, 1587, 1435, 1307, 1274, 1136, 825. ^{1}H-NMR (acetone-d_6, 500 MHz): δ: 7.77 (ddd, *J*=8.75, 2.60, 1.9 Hz, 2H), 7.59 (ddd, *J*=8.75, 2.60, 1.90 Hz, 2H), 6.76 (ddd, *J*=8.8, 2.25, 0.45 Hz, 2H), 6.71 (ddd, *J*=8.9, 2.25, 1.15 HZ, 2H), 5.42 (w. s, 2H), 2.82 (w. s, 20H), 2.79 (w. s, 6H), 1.26 (w. s, 4H). ^{13}C-NMR (acetone-d_6, 125 MHz) δ: 168.7, 152.5, 145.6, 130.2, 129.5, 123.6, 78.3, 53.0, 51.0, 32.9, 29.3, 24.2, 13.6.

In silico prediction of physicochemical and pharmacokinetic properties. Bioactivity and cheminformatics prediction (including absorption, distribution, metabolism, excretion, and toxicity, pharmacokinetic and medicinal chemistry properties) were calculated using canonical simplified molecular-input line-entry system sequences retrieved from the pdb files of the density functional theory-optimized structures using Avogadro software version 1.2.0 (https://avogadro.uptodown.com/windows). The chemical space analysis was focused on four physicochemical properties of pharmaceutical relevance, molecular weight, topological polar surface area (TPSA), partition coefficient (cLogP) and solubility Log S (ESOL), which were predicted using the SwissADME web tool (http://www.swissadme.ch/index.php; access date: 02 March 2023). Bioavailability radars and Lipinski's (16), Ghose's (17), Veber's (18), Egan's (19) and Muegge's (20) rules were also calculated using SwissADME.

Biology

Reagents. Stock solutions of DDS and its synthetic derivative were prepared in dimethyl sulfoxide (DMSO) at a concentration of 1 mg/ml, then stored at -20˚C. The final concentrations of DMSO were below 0.1% (v/v) for all experiments. The reagent ethanol (MilliporeSigma) was included as a deathtime control using concentrations ranging from 4-13% (v/v).

Cell cultures and growth conditions. The human metastatic prostate carcinoma (DU145) and the human adenocarcinoma cervix (HeLa) cell lines were obtained from American Type Culture Collection with the following registration numbers: HTB-81 and CRM-CCL-2, respectively. These were grown in an adherent monolayer culture in Dulbecco's Minimum Essential Medium (DMEM) and both were supplemented with 10% heat-inactivated fetal bovine serum (FBS), 1% L-glutamine and 1% penicillin/streptomycin in a humidified atmosphere (5% CO_2; 37˚C). All media and supplements were purchased from MilliporeSigma. The primary dermal fibroblast cell line-HDFa was obtained from ATCC with the registration number PCS-201-012 and it was used to validate the cytotoxicity results using concentrations ranging from 12.5-100 μM.

Cell viability assay. 3-(4,5-Dimethylthiazol-2-yl)-2,5-diphenyltetrazolium bromide (MTT; Invitrogen; Thermo Fisher Scientific, Inc.) was used to measure the cytotoxicity of the tested compounds. Briefly, the cells were seeded in 96-well plates (20,000 cells/well). Following overnight incubation at 37˚C, the cells were treated with or without the tested compounds (at different concentrations ranging from 0.01-100 μM). Untreated cells containing fresh medium were used as lifetime controls and fresh medium alone was used as a blank. Following the 24- and 48-h treatments, the cells were incubated with MTT at a final concentration of 0.5 mg/ml for 2.5 h in 5% CO_2 at 37˚C. Finally, a solution of 100% DMSO (50 μl) was added to solubilize the purple formazan. The

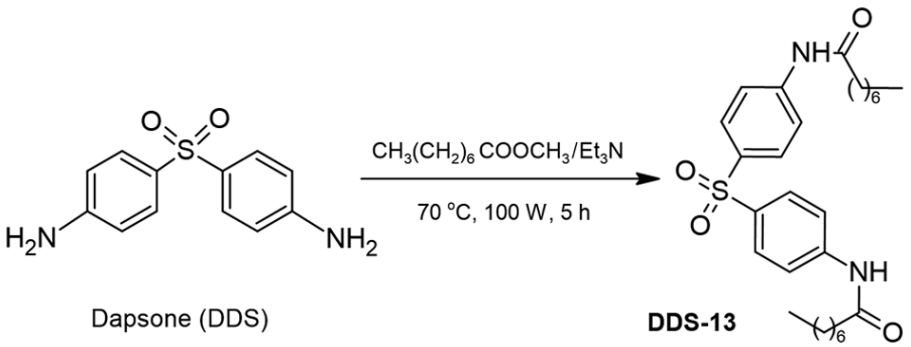

Figure 1. Synthesis of DDS-13. Figure constructed in ChemSketch software version 2.0 (https://www.acdlabs.com/resources/free-chemistry-software-apps/chemsketch-freeware/) using the ACS style. ACS, American Chemical Society; DDS, dapsone.

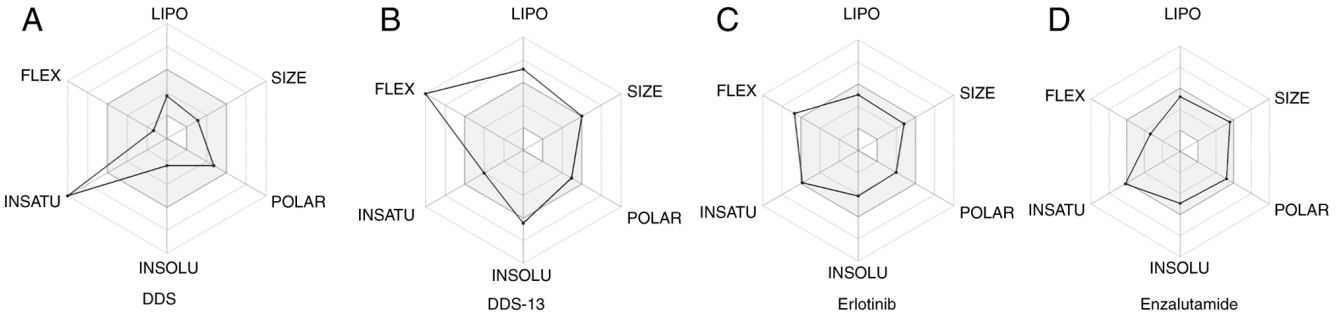

Figure 2. Bioavailability radars for (A) DDS, (B) DDS-13, (C) erlotinib and (D) enzalutamide. The optimal range for each property (size, lipophilicity, solubility, polarity and flexibility) are represented by the gray area. DDS, dapsone.

absorbance of the converted dye was measured the next day at 570 nm using a spectrophotometer (Smartreader 96; Accuris Instruments). MTT data are expressed as the mean ± SD of at least three independent experiments (triplicates). The absorption readings were converted into percent of cells. The IC_{50} values representing the concentrations (μM) of the tested compounds reducing the cell viability by 50%, were calculated using an IC_{50} calculator, AAT Bioquest (https://www.aatbio.com/tools/ic50-calculator).

Morphological evaluation of cell cultures. Papanicolaou's stain was used to morphologically evaluate the possible type of cell death induced by each of the treatments (DDS and DDS-13) in the different cell lines (HDFa, DU145 and HeLa). Untreated cells were used as controls and cells treated with DDS and DDS-13 at concentrations of 0.01 and 100 μM were assessed. A total of 20,000 cells per well were plated on Chamber Slide devices (Nunc Lab-Tek II, Thermo Fisher Scientific, Inc.) and incubated at 37˚C for 48 h. The cells were then fixed in 96% ethanol and stained with Papanicolaou according to a modified procedure (21): Cells were stained with hematoxylin (MilliporeSigma) for 2 min, followed by two slow dips under tap water, a slow dip under 1% ammoniacal water and two slow dips under tap water, and then stained with OG-6 (MilliporeSigma) for 2 min and with EA-50 (Merck KGaA) for 2 min, followed by a slow dip under 96% ethanol and another under 100% ethanol. The samples were cleared in xylene (MilliporeSigma) and mounted with rapid mounting medium (Entellan; MilliporeSigma). These were observed under a light microscope (Primo Star; Zeiss AG) and analyzed by a specialized pathologist.

Statistical analysis. The comparison of the means was performed using Student's t-test and a one-way ANOVA (with Bonferroni's post-hoc test) with Sigma Plot v12.5 (Systat Software Inc.) and GraphPad Prism (GraphPad Software; Dotmatics). Data are presented as the mean ± standard deviations. $P<0.05$ was considered to indicate a statistically significant difference.

Results

Chemistry

Chemical synthesis. DDS-13 was obtained through the condensation of DDS and methyl caprylate, using a combination of triethylamine (Et_3N) and acetone as the solvent, with reaction times of up to 5 h under microwave irradiation. The compound was obtained as a white solid with a 75% yield. The derivative structure was confirmed through NMR and FT-IR (Figs. S3-S5). Fig. 1 shows the chemical structures of the obtained compounds.

In silico analysis. The SwissADME web tool (22) was used as a prediction model for the identification of the physicochemical and pharmacokinetic properties of DDS-13 (see details in the Methods section). The bioavailability radars for DDS (Fig. 2A) and the reference drugs erlotinib (Fig. 2C) and enzalutamide (Fig. 2D) were shown to be outside the optimal ranges for one physicochemical property: DDS and enzalutamide in saturation and erlotinib in flexibility. The synthetic derivative DDS-13 (Fig. 2B) was shown to be outside of the optimal ranges for three physicochemical properties: lipophilicity, solubility and flexibility. Table I shows the structural and

Table I. Structural and physicochemical properties of DDS, DDS-13, erlotinib and enzalutamide compounds.

Compound	Molecular weight, g/mol	TPSA Å^2	Log $P_{o/w}$		Log S (ESOL)	HBAs	HBDs	Rotatable bonds	Drug-likeness[a]					Bioavailability score
			WLOGP	MLOGP					Lipinski	Ghose	Veber	Egan	Muegge	
DDS	248.3	94.56	0.97	1.87	-2.38	2	2	2	0	0	0	0	0	0.55
DDS-13	500.69	100.72	7.06	4.55	-6.46	4	2	18	2	4	1	1	2	0.17
Erlotinib	393.44	74.73	3.31	1.48	-4.11	6	1	10	0	0	0	0	0	0.55
Enzalutamide	464.44	108.53	3.61	2.73	-4.94	7	1	5	0	0	0	0	0	0.55

[a]Number of rule violations. DDS, dapsone; TPSA, topological polar surface area; Log $P_{o/w}$, octanol/water partition coefficient; WLOGP, Wildman octanol-water partition coefficient; MLOGP, Moriguchi octanol-water partition coefficient; ESOL, Log S solubility; HBAs, H-bond acceptors; HBDs, H-bond donors.

physicochemical properties, where only the DDS-13 derivative slightly exceeded the molecular weight limits (>500 g/mol) according to the reference established by the prediction model. All compounds possessed an adequate TPSA (<130 Å^2) for membrane permeation. As for the ESOL, it was established that the reference and DDS drugs showed improved solubility than DDS-13.

Among the pharmacokinetic properties (Table II), it was observed that the octanol/water partition coefficient (cLog$P_{o/w}$ or WLOGP), as considered by Egan, or the Moriguchi octanol-water partition coefficient, as considered by Lipinski, demonstrated that the reference and DDS drugs may have exhibited improved gastrointestinal (GI) absorption than the DDS-13 derivative. Erlotinib is the only reference drug with permeability to the blood-brain barrier (BBB).

Biology

In vitro analysis. For the evaluation of the cytotoxic effects of DDS and its synthetic derivative DDS-13, the experimental study was performed on cancer cell lines of solid prostate (DU145) and cervical (HeLa) tumors. In the first stage, to evaluate whether there were differences between the durations of exposition to the treatment, DU145 and HeLa cells were exposed to 0.01, 0.1, 1, 10 and 100 μM of DDS (T) and the cell viability was determined at 24 and 48 h. To determine the percentage of cell viability, the optical density (OD), a lifetime control (CNT) and a blank (B) were used. The formula of cell viability (%)=$(OD_T-OD_B)/(OD_{CNT}-OD_B)$ x100 was used for the determination. Table III shows the comparison of the cell viability percentage with DDS at various concentrations at the 24- and 48-h time points. There were no significant differences in the different concentrations between the two time points (P>0.05), except for the 100 μM concentration (P=0.03). In general, the highest cytotoxic effect was observed at 48 h. Based on these first results, subsequent analyses were performed to evaluate the different concentrations of each compound at only at the 48-h time point.

Table IV shows a comparison of the cell viability percentages of the different concentrations (0.01-100 μM) for both DDS and DDS-13, in DU145 and HeLa cell lines at the 48-h time point. A comparison of the different concentrations of each compound showed significant differences in the two cell lines used (P<0.05). In the DU145 cell line, DDS-13 reduced the cell viability percentage, unlike the DDS, at the following concentrations: 0.01 μM (44.2%), 0.1 μM (11.2%), 1 μM (26.5%), 10 μM (17.3%) and 100 μM (42.6%). There were significant differences between DDS and DDS-13 (Fig. 3A) at the concentrations of 0.01 μM (P=0.005) and 100 μM (P=0.003). The mean inhibitory concentration (IC_{50}) is also highlighted in Table IV and was calculated at 11.11 for DDS and 19.06 μM for DDS-13. In the HeLa cell line, the rates of reduction in the cell viability percentage at the different concentrations of DDS-13 were as follows: 0.01 μM (23%), 1 μM (18.1%), 10 μM (6.2%) and 100 μM (29.7%). At the 0.1 μM concentration, there was no reduction in the cell viability percentage. A significant difference between DDS and DDS-13 (Fig. 3B) at a concentration of 100 μM was also observed (P=0.035). The IC_{50} for DDS was 13.07 μM and that for DDS-13 was 67.91 μM. Overall, the greatest decrease in cell viability percentage for both DDS and DDS-13 was observed at 100 μM in both cell lines.

Table II. Pharmacokinetic properties and medicinal chemistry of DDS, DDS-13, Erlotinib and Enzalutamide compounds.

	Pharmacokinetics								Medicinal chemistry		
Compound	GI absorption	BBB permeant	P-gp substrate	CY1A2 inhibitor	CYP2C19 inhibitor	CYP2C9 inhibitor	CYP2D6 inhibitor	CYP3A4 inhibitor	PAINS	Brenk	Lead-likeness
DDS	High	No	No	No	No	No	No	No	0	1	1
DDS-13	Low	No	No	No	Yes	Yes	No	Yes	0	0	3
Erlotinib	High	Yes	No	Yes	Yes	Yes	Yes	Yes	0	1	2
Enzalutamide	High	No	No	No	Yes	Yes	No	Yes	0	1	2

DDS, dapsone; GI, gastrointestinal; BBB, blood-brain barrier; PAINS, pan assay interference compounds.

Table III. Analysis of the cytotoxic concentrations between the time points of 24 and 48 h with the DDS compound in DU145 and HeLa cell lines.

		Cell viability for different concentrations of DDS, %					
Cell line	Time (h)	0.01 μM	0.1 μM	1 μM	10 μM	100 μM	P-value
DU145	24	93.4±4.9	70.3±3.3	86.3±5.0	72.8±3.7	60±2.9	0.002[a]
	48	110.4±3.3	77.7±6.5	106.3±6.6	83.0±7.6	59.1±4.8	0.002[a]
		P=0.057	P=0.29	P=0.078	P=0.234	P=0.843	
HeLa	24	95.4±3.3	78.2±3.6	98.3±6.6	81.0±4.8	68.9±2.9	0.005[a]
	48	103.0±3.5	69.0±6.5	93.8±6.5	74.3±7.9	34.5±8.0	<0.001[a]
		P=0.16	P=0.224	P=0.564	P=0.414	P=0.03[a]	

[a]P<0.05. Data are represented as cell viability percentage (mean ± SD). One-way ANOVA with Bonferroni's post-hoc test, t-test, 95% CI. DDS, dapsone.

Table IV. Concentration analysis of DDS and DDS-13 compounds in DU145 and HeLa cell lines at the 48-h time point.

		Cell viability for different concentrations of DDS, %						
Cell line	Treatment	0.01 μM	0.1 μM	1 μM	10 μM	100 μM	P-value	IC_{50} (μM)
DU145	DDS	110.4±3.3	77.7±6.5	106.3±6.6	83.0±7.6	59.1±4.8	0.002[a]	11.11
	DDS-13	66.2±2.5	66.5±3.8	79.8±8.0	65.7±9.6	16.5±10.1	0.002[a]	19.06
		P=0.005[a]	P=0.171	P=0.070	P=0.185	P=0.033[a]		
HeLa	DDS	103.0±3.5	69.0±6.5	93.8±6.5	74.3±7.9	34.5±8.0	<0.001[a]	13.07
	DDS-13	80.0±7.3	89.2±9.1	75.7±7.6	68.1±10.1	4.8±0.8	<0.001[a]	67.91
		P=0.058	P=0.127	P=0.125	P=0.567	P=0.035[a]		

[a]P<0.05. Data are represented as the cell viability percentage (mean ± SD). One-way ANOVA with Bonferroni's post-hoc test, t-test, 95% CI. DDS, dapsone.

To evaluate the cytotoxicity of the compounds of interest (DDS and DDS-13) on non-cancerous cells, the primary dermal fibroblast cell line (HDFa) was used due to its availability in the Molecular Medicine Laboratory (Autonomous University of Zacatecas, Zacatecas, Mexico). The studied concentrations included concentrations below and above the IC_{50} calculated previously for each cancer cell line. These were 12.5, 25, 50 and 100 μM. Fig. 3C shows the results obtained for the cell viability percentage with each of the compounds in the HDFa cell line. It was observed that there was cytotoxicity with DDS-13 at concentrations of 50 μM (reduction of 64.2% in cell viability) and 100 μM (reduction of 83.6% in cell viability). It was observed that there was no cytotoxicity with DDS at most concentrations, except for 12.5 μM (a reduction of 54.4% in cell viability). There were significant differences between DDS and DDS-13 at all tested concentrations, but

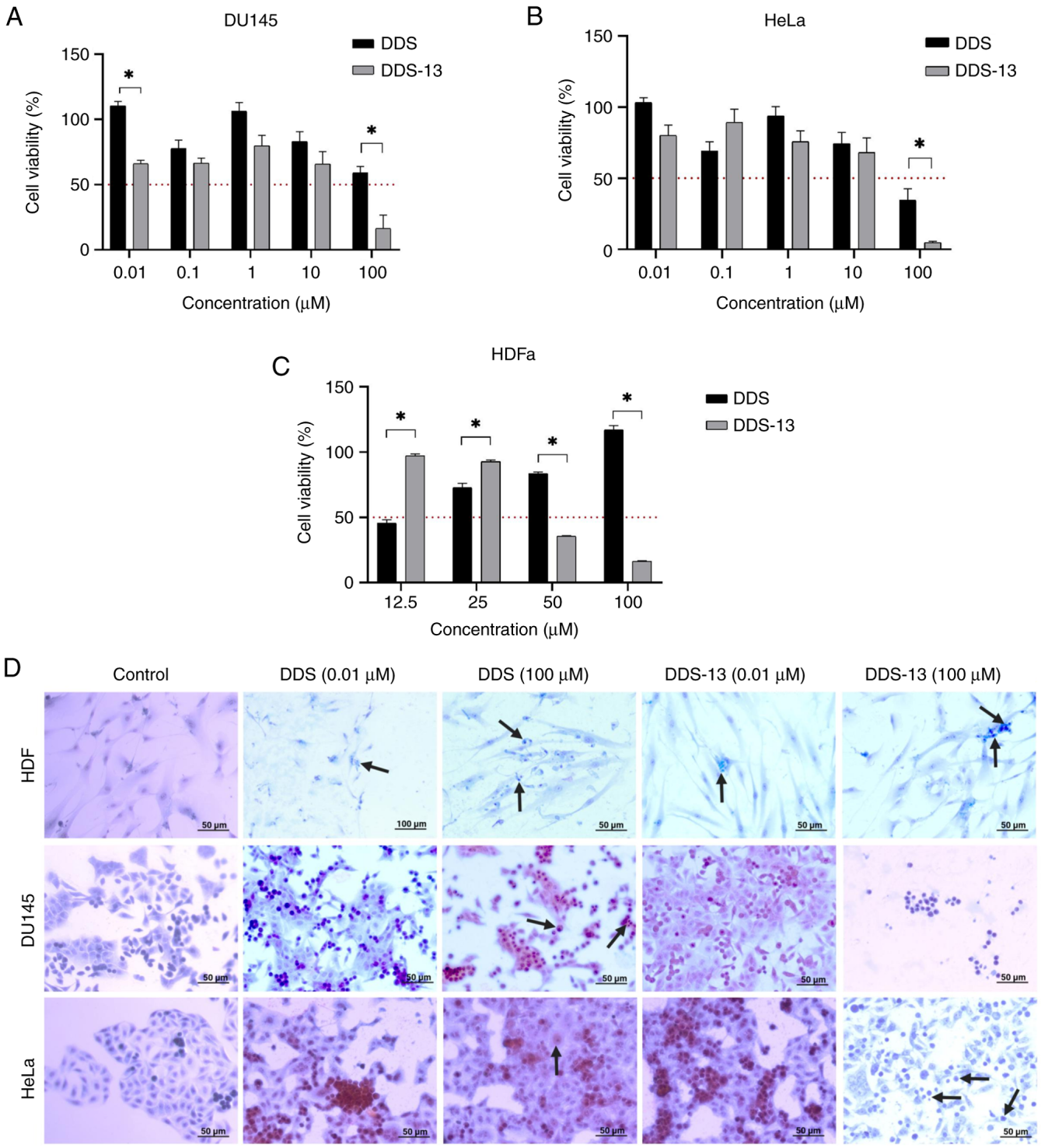

Figure 3. Cytotoxicity of DDS and DDS-13 in DU145, HeLa and HDFa cell lines. Comparison of the cell viability percentages (y-axis) between DDS and DDS-13 (mean ± SD) at concentrations from 0.01 to 100 μM (x-axis) in (A) DU145 and (B) HeLa cell lines. (C) Comparison of the cell viability percentages (y-axis) between DDS and DDS-13 (mean ± SD) at the different concentrations (x-axis) in the HDFa cell line. The 50 percent reduction in cell viability is represented by the dotted line (red). Data were evaluated using Student's t-test. *P<0.05. (D) Cell death in HDF, DU145 and HeLa cell lines by Papanicolaou staining. Morphological comparison of untreated (control) and treated cell lines with DDS and DDS-13 at 0.01 and 100 μM concentrations. Arrows indicate foci of cell death by apoptosis. DDS, dapsone.

mostly at concentrations of 50 and 100 μM (P<0.001). The IC_{50} for DDS-13 was 40.92 μM.

Papanicolaou staining was used to assess the type of cell death in cells treated with DDS and DDS-13. No cell death was observed in untreated cells, as opposed to in treated cells (Fig. 3D). In cancer cells (DU145 and HeLa) treated with DDS (0.01 and 100 μM), hyperchromatic nuclei with sparse dense cytoplasm were observed, suggesting cell death by apoptosis. The process was more evident at higher concentrations. The same effect occurred with cancer cells treated with DDS-13, where the foci of cell death by apoptosis were greater and the cell density was considerably lower, specifically at the 100 μM

concentration. In non-cancerous cells treated with DDS and DDS-13, some foci of cell death by apoptosis were also observed in a smaller proportion; however, cell density did not decrease with any of the treatments.

Discussion

Globally, cancer represents a major health problem due to its high mortality rate (3). In terms of drug discovery, drug repositioning has gained increasing importance because it helps to circumvent preclinical optimization (23). The present study focused on evaluating DDS and its synthetic derivative, DDS-13, in an *in vitro* study to contribute to the proposal of candidate treatments with potential cytotoxic effects on cancer cells. To date, there is little information on the effects of DDS and its synthetic derivatives on cancer. DDS is chemically known as 4,4'-diaminodiphenylsulfone; it is an old antibiotic drug that belongs to the group of synthetic sulfones (24). Due to its side effects, namely, methemoglobinemia and hemolytic anemia, DDS is mainly used in topical preparations for the treatment of dermatological diseases (7). One strategy for the structural modification of drugs containing amine functionalities, as is the case for DDS, consists of derivatization to imines or amides. From a synthetic point of view, the imine group has the advantage of being easily accessible, which can improve biological activity and solubility compared with precursor amines (25,26). In the present study, DDS-13 was selected from a group of synthetic derivatives of DDS obtained by our working group. This derivative has not been functionally or biologically tested to evaluate its potential pharmacological properties against cancer. DDS and its synthetic derivative DDS-13 were evaluated *in silico,* and they were compared with two reference drugs approved by the US Food and Drug Administration (FDA): Erlotinib and enzalutamide, which have antineoplastic activities in cervical (27) and prostate cancer (28), the two types of cancer evaluated in the present study. In the results of the *in silico* analysis, it was observed that DDS-13 had more physicochemical properties out of range than DDS and the reference drugs (Table I). Erlotinib and DDS-13 were shown to be outside of the optimal ranges, with rotatable bonds greater than nine in the flexibility property and with DDS and enzalutamide in the saturation property. Other properties of DDS-13 which were found to be out of range were lipophilicity (WLOGP=7.06) and solubility (Log S=-6.46). Drug likeness qualitatively assesses the likelihood of a molecule becoming an oral drug with respect to its bioavailability. This section gives access to five different rule-based filters (Lipinski, Ghose, Veber, Egan and Muegge) with different ranges of properties that define a molecule as drug-like. DDS-13 exhibited violations in these filters, unlike DDS or the reference drugs. The present study studied the pharmacokinetic properties and DDS-13 and none of the studied molecules crossed the BBB, except for erlotinib (Table II). In medicinal chemistry, the Brenk filters helped to define the lead-likeness criteria in order to establish whether a molecule was suitable for optimization. The present study observed that all compounds presented violations in at least one of the filters, which was more evident with DDS-13. The predictions for BBB permeation and passive human gastrointestinal absorption consisted of the readout of the BOILED-Egg model (29) (Fig. S1). It was observed that DDS-13 demonstrated less bioavailability by oral absorption than the other compounds. DDS had higher bioavailability by gastrointestinal absorption than the reference drug enzalutamide. Erlotinib, enzalutamide and DDS are classified as class II drugs according to the BCS, with low solubility and high permeability (12). However, these rules of thumb only consider a passive diffusion mechanism through the GI barrier; therefore, the limitations of our derivative can be solved by a different administration route, through formulation or by considering an ATP-dependent transport.

In the *in vitro* model, the cytotoxic effects of DDS and DDS-13 were demonstrated at concentrations of 10 and 100 μM in the DU145 and HeLa cell lines, with the greatest cytotoxic effect observed at a concentration of 100 μM (cell viability reduction of >50%). The synthetic derivative DDS-13 showed greater cytotoxic effects than DDS in both the DU145 (3.5x reduction in cell viability) and HeLa (7x reduction in cell viability) cell lines ($P<0.05$). In the HeLa cell line, the cytotoxic effect was more pronounced. This correlated with the result seen with Papanicolaou staining, where morphological cell death at the 100 μM concentration was higher and cell density was lower (Fig. 3D). Then, four concentrations (12.5-100 μM) above the IC_{50} concentrations previously seen in cancer cell lines were included to evaluate the cytotoxicity on a non-cancerous cell line (HDFa). The results indicated that DDS-13 had no cytotoxic effect on this cell line in a concentration range from 12.5 to 25 μM ($IC_{50=}$40.92 μM). The IC_{50} concentration for HDFa cells was >IC_{50} concentration seen in the DU145 cell line (19.06 μM). These results suggested that DDS-13 appeared to be a good candidate for additional assays due to its cytotoxic effect only on the DU145 cell line and not on primary fibroblasts within the aforementioned range of concentrations. A limitation of the present study was that it did not complement the cytotoxic effect of DDS-13 on DU145 and HeLa cells in the concentration range of 12.5-25 μM; however, these evaluations can be integrated into further studies. The significant killing of cancer cells by DDS-13 was observed at a concentration of 100 μM; at this concentration, the survival of non-cancerous cells was similar to that of cancerous cells (DU145 cells). The same was observed morphologically by Papanicolaou staining (Fig. 3D) and cell death at this concentration was higher.

Therefore, it may be pertinent to study cell survival by considering a wider range of concentrations (10-100 μM) in both cancerous and non-cancerous cells to determine whether there is a concentration range that is more cytotoxic to cancer cell than non-cancer cell lines. Regarding DDS, the IC_{50} calculated in the HeLa cell line (13.07 μM) was lower than the IC_{50} concentration observed in the HDFa cells. The high DDS cytotoxic effect observed on HeLa cells (Fig. 3B) positions DDS as an improved candidate compared with DDS-13 for preclinical studies of cervical cancer, because it had no cytotoxic effect on HDFa cells in a range of concentrations from 25-100 μM. Similarly, for prostate cancer, DDS showed an IC_{50} of 11.11 μM in the DU145 cell line, which is well below the concentrations tested as non-cytotoxic for HDFa (25, 50 and 100 μM). These results may be considered as a basis on which to increase the DDS concentrations to 100 μM, with the object of evaluating whether its specific cytotoxic effect on prostate tumor cells would be greater. In HDFa cells, DDS-13

showed a safety margin in the normal HDFa cells only between 12.5-50 μM, compared with the dose-dependent selectivity of DDS. However, morphologically, it is important to stress that with both DDS and DDS-13, cell density was not significantly reduced, as was observed in cancer cell lines (Fig. 3D). The antitumor effects of DDS and/or DDS-13 are not well known. A study conducted in 2016 by Boccellino *et al* (9) highlighted that DDS could present an antitumor effect by blocking IL8 and reducing growth factors, such as the VEGF, in an *in vitro* model; however, this mechanism has not been proved. Regarding synthetic DDS derivatives, three studies have been conducted, one of them by Karpel-Massler *et al* (2017) (11), which highlights the reduction in anchorage-independent growth, the decrease in clonogenic survival and the reduction of directed migration in a glioblastoma cell line. The derivatives evaluated in that study were different from those evaluated in the present study. The 2017 study (11) suggested possible effects of DDS in cancer; however, it did not demonstrate these mechanisms. The concentrations evaluated in this previous study were similar to those evaluated in the present study. Pillai *et al* (30) evaluated synthetic DDS derivatives different from those in the present study, as well as their *in vitro* anticancer activity against the Hep G2 (hepatocellular carcinoma) and C6 (glioblastoma) cell lines, suggesting specificity of the compounds for cancer cells over normal liver cells. They proposed apoptotic cell death as a mechanism of cytotoxic action for their derivatives. The present study decided to include Papanicolaou staining to morphologically compare cells with DDS and DDS-13 (0.01 and 100 μM); the findings indicated that the likely mechanism of cell death is given by apoptosis due to specific features, such as shrinkage of the nuclei, sparse dense cytoplasm, hyperchromatic nuclei and signs of pre-apoptotic bodies. These results need to be validated with additional studies.

In vivo studies have shown that inhibition of CYP2C19, CYP2C9 and CYP3A4 isoenzymes, as seen in the present *in silico* analysis with DDS-13, is one major cause of pharmacokinetic-related drug-drug interactions (31). These lead to various adverse effects, such as toxicity due to decreased clearance and accumulation of the drug or its metabolites. These cytochromes have been reported to be differentially expressed in types of cancer (32,33). Additional studies will be needed in order to confirm the DDS-13 effect of these isoenzymes. Another study by Guzmán-Ávila *et al* (34) showed that the evaluated synthetic derivatives demonstrated antioxidant activity in an *in silico* model. Synthetic derivatives are different from the one evaluated in the present study. Regarding analyses of the structure of DDS-13, there are only two early studies, which reported similar, but not the same, structural characteristics of the compound synthesis and these did not address anything about their possible effects (35,36). In the same manner, this synthetic derivative has not been evaluated in cancer. Therefore, DDS-13 has not previously been synthesized as it was in the present study, nor has it been biologically evaluated. From the results of the present study, cytotoxic effects of DDS and DDS-13 were demonstrated on DU145 and HeLa cell lines, supporting the antitumor properties of these molecules specifically for prostate or cervical tumors. In accordance with the differential effects which were identified, it is highly probable that the chemical structures of each of them are involved in their different mechanisms of action.

Finally, is important to note that the present study observed a non-linear trend at low concentrations (0.01 and 0.1 μM) of DDS and DDS-13 in both cancer cell lines which were evaluated. These trends were contrary to those observed from the 1 μM concentration level and above. In principle, this finding would rule out these concentrations for the evaluation of the cytotoxic effect; however, since it was a reproducible finding in both cell lines, with both compounds and during all the experiments, additional viability assays were performed in which ethanol dilutions (4-13 μM) were included for quality control of the cytotoxic assays. However, in future studies it would be desirable to include chemotherapeutic drugs, such as enzalutamide, as a cytotoxicity control for comparative purpose. On the three cell lines which were used, a dose-dependent cytotoxic effect was observed with ethanol (Fig. S2). This effect was different from that observed with DDS-13 and DDS in the cancer cell lines. Exactly what occurs at these concentrations in the cancer cell lines included in the present study is unclear, but different mechanisms of action are probably triggered due to the chemical and physicochemical properties of each compound. Additional studies will be needed in order to identify whether the effect observed in our study corresponds to dual effects or mechanisms of DDS and DDS-13 at low concentrations, or even these effects are maintained with other DDS derivatives.

In conclusion, DDS and its synthetic derivative DDS-13 showed cytotoxic effects in *in vitro* models of prostate and cervical cancer. DDS-13 showed cytotoxic effects in the DU145 cell line, proving to be a good candidate for prostate cancer, with no cytotoxic effect in non-cancerous cells. DDS showed a cytotoxic effect in both the DU145 and HeLa cell lines, proving to be a good candidate for both prostate and cervical cancer. The present study demonstrated improved results in cervical cancer cells, without a cytotoxic effect on non-cancerous cells. DDS-13 presented different pharmacokinetic properties compared with DDS, making it a new and interesting candidate for evaluation in preclinical models of cancer treatment. The proposal of this synthetic derivative could contribute to the discovery of new cancer treatments to counteract the adverse effects and costs of current treatment schemes. Further *in vitro* and *in vivo* studies are needed in order to elucidate a possible mechanism of action and to validate the antitumor effect.

Acknowledgements

Not applicable.

Funding

The present study was funded by the Academic Unit of Human Medicine and Health Sciences of the Autonomous University of Zacatecas and by CONACYT via a scholarship fund (grant no. 2021-000018-02NACF-15274).

Availability of data and materials

The datasets used and/or analyzed during the current study are available from the corresponding author on reasonable request.

Authors' contributions

MMF and VF designed the study. GC, IG, VF, RM, MD and MMV performed the experiments and analyzed the data. ID and IR contributed substantially to the data interpretation and participated in critical manuscript revision. GC, VF, IG, MMF wrote the manuscript. GC, MMF, MC, ID and IR searched the literature and revised the manuscript. All authors read and approved the final manuscript. MMF and VF confirm the authenticity of all the raw data.

Ethics approval and consent to participate

Not applicable.

Patient consent for publication

Not applicable.

Competing interests

The authors declare that they have no competing interests.

References

1. Catherine Sánchez N: Knowing and understanding the cancer cell: physiopathology of cancer. Rev Méd Clin Las Condes 24: 553-562, 2013.
2. World Health Organization (WHO): International Agency for Research on Cancer. WHO, Geneva, 2020. https://gco.iarc.fr/today/online-analysis-multi-bars.
3. Ghose S, Radhakrishnan V and Bhattacharya S: Ethics of cancer care: Beyond biology and medicine. Ecancermedicalscience 13: 911, 2019.
4. Jarada TN, Rokne JG and Alhajj R: A review of computational drug repositioning: Strategies, approaches, opportunities, challenges, and directions. J Cheminform 12: 46, 2020.
5. Ross CM: The treatment of acne vulgaris with dapsone. Br J Dermatol 73: 367-370, 1961.
6. Reunala T, Hervonen K and Salmi T: Dermatitis herpetiformis: An update on diagnosis and management. Am J Clin Dermatol 22: 329-338, 2021.
7. Wozel G and Blasum C: Dapsone in dermatology and beyond. Arch Dermatol Res 306: 103-124, 2014.
8. Molinelli E, Paolinelli M, Campanati A, Brisigotti V and Offidani A: Metabolic, pharmacokinetic, and toxicological issues surrounding dapsone. Expert Opin Drug Metab Toxicol 15: 367-379, 2019.
9. Boccellino M, Quagliuolo L, Alaia C, Grimaldi A, Addeo R, Nicoletti GF, Kast RE and Caraglia M: The strange connection between epidermal growth factor receptor tyrosine kinase inhibitors and dapsone: From rash mitigation to the increase in anti-tumor activity. Curr Med Res Opin 32: 1839-1848, 2016.
10. Kanoh S, Tanabe T and Rubin BK: Dapsone inhibits IL-8 secretion from human bronchial epithelial cells stimulated with lipopolysaccharide and resolves airway inflammation in the ferret. Chest 140: 980-990, 2011.
11. Karpel-Massler G, Kast RE, Siegelin MD, Dwucet A, Schneider E, Westhoff MA, Wirtz CR, Chen XY, Halatsch ME and Bolm C: Anti-glioma activity of dapsone and its enhancement by synthetic chemical modification. Neurochemical Res 42: 3382-3389, 2017.
12. Lindenberg M, Kopp S and Dressman JB: Classification of orally administered drugs on the World Health Organization model list of essential medicines according to the biopharmaceutics classification system. Eur J Pharm Biopharm 58: 265-278, 2004.
13. Gallardo CA, Fan BE, Lim KGE and Kuperan P: Chronic dapsone use causing methemoglobinemia with oxidative hemolysis and dyserythropoiesis. Am J Hematol 96: 1715-1716, 2021.
14. Vogel AI, Furniss BS, Hannaford AJ, Smith PW and Tatchell AR: Vogel's textbook of practical organic chemistry. 5th edition. John Wiley & Sons, New York, NY, pp395-469, 1989.
15. Lidstrom P, Tierney J, Wathey B and Westman J: Microwave assisted organic synthesis-a review. Tetrahedron 57: 9225-9283, 2001.
16. Lipinski CA, Lombardo F, Dominy BW and Feeney PJ: Experimental and computational approaches to estimate solubility and permeability in drug discovery and development settings. Adv Drug Deliv Rev 46: 3-26, 2001.
17. Ghose AK, Viswanadhan VN and Wendoloski JJ: A knowledge-based approach in designing combinatorial or medicinal chemistry libraries for drug discovery. 1. A qualitative and quantitative characterization of known drug databases. J Comb Chem 1: 55-68, 1999.
18. Veber DF, Johnson SR, Cheng HY, Smith BR, Ward KW and Kopple KD: Molecular properties that influence the oral bioavailability of drug candidates. J Med Chem 45: 2615-2623, 2002.
19. Egan WJ, Merz KM Jr and Baldwin JJ: Prediction of drug absorption using multivariate statistics. J Med Chem 43: 3867-3877, 2000.
20. Muegge I, Heald SL and Brittelli D: Simple selection criteria for drug-like chemical matter. J Med Chem 44: 1841-1846, 2001.
21. Sathawane P, Kamal MM, Deotale PR and Mankar H: Nuances of the Papanicolaou stain. Cytojournal 19: 43, 2022.
22. Swiss Institute of Bioinformatics (SIB): SwissADME. http://www.swissadme.ch/index.php#.
23. March-Vila E, Pinzi L, Sturm N, Tinivella A, Engkvist O, Chen H and Rastelli G: On the integration of in silico drug design methods for drug repurposing. Front Pharmacol 8: 298, 2017.
24. do Amaral LH, do Carmo FA, Amaro MI, de Sousa VP, da Silva L, de Almeida GS, Rodrigues CR, Healy AM and Cabral LM: Development and characterization of dapsone cocrystal prepared by scalable production methods. AAPS PharmSciTech 19: 2687-2699, 2018.
25. Jornada DH, dos Santos Fernandes GF, Chiba DE, de Melo TR, dos Santos JL and Chung MC: The prodrug approach: A successful tool for improving drug solubility. Molecules 21: 42, 2015.
26. Day TP, Sil D, Shukla NM, Anbanandam A, Day VW and David SA: Imbuing aqueous solubility to amphotericin B and nystatin with a vitamin. Mol Pharm 8: 297-301, 2011.
27. Schilder RJ, Sill MW, Lee YC and Mannel R: A phase II trial of erlotinib in recurrent squamous cell carcinoma of the cervix: A gynecologic oncology group study. Int J Gynecol Cancer 19: 929-933, 2009.
28. Davis ID, Martin AJ, Stockler MR, Begbie S, Chi KN, Chowdhury S, Coskinas X, Frydenberg M, Hague WE, Horvath LG, *et al*: Enzalutamide with standard first-line therapy in metastatic prostate cancer. N Engl J Med 381: 121-131, 2019.
29. Daina A and Zoete V: A BOILED-Egg to predict gastrointestinal absorption and brain penetration of small molecules. ChemMedChem 11: 1117-1121, 2016.
30. Pillai V, Kadu R, Buch L and Singh VK: Derivatives of dapsone (dap): Synthesis and study on in vitro anticancer activity and DNA laddering against Hep G2 and C6 human cancer cell lines. ChemistrySelect 2: 4382-4391, 2017.
31. Huang SM, Strong JM, Zhang L, Reynolds KS, Nallani S, Temple R, Abraham S, Habet SA, Baweja RK, Burckart GJ, *et al*: New era in drug interaction evaluation: US food and drug administration update on CYP enzymes, transporters, and the guidance process. J Clin Pharmacol 48: 662-670, 2008.
32. Uetrecht J, Zahid N, Shear NH and Biggar WD: Metabolism of dapsone to a hydroxylamine by human neutrophils and mononuclear cells. J Pharmacol Exp Ther 245: 274-279, 1988.
33. Tian D and Hu Z: CYP3A4-mediated pharmacokinetic interactions in cancer therapy. Curr Drug Metab 15: 808-817, 2014.
34. Guzmán-Ávila R, Avelar M, Márquez EA, Rivera-Leyva JC, Mora JR, Flores-Morales V and Rivera-Islas J: Synthesis, in vitro, and in silico analysis of the antioxidative activity of dapsone imine derivatives. Molecules 26: 5747, 2021.
35. Zasosov VA: Diacyl derivatives of bis (4-aminophenyl) sulfone. Zhurnal Obshchei Khimii 17: 471-476, 1947.
36. Hensel; Walter; Buechner O, inventor Polyolefin molding compositions containing diamides, 1967.